Published OnlineFirst August 10, 2015; DOI: 10.1158/0008-5472.CAN-15-0380

Therapeutics, Targets, and Chemical Biology

Cancer Research

Genome-Wide Identification and Characterization of Novel Factors Conferring Resistance to Topoisomerase II Poisons in Cancer

Ruud H. Wijdeven[1], Baoxu Pang[1], Sabina Y. van der Zanden[1], Xiaohang Qiao[1], Vincent Blomen[2], Marlous Hoogstraat[3,4], Esther H. Lips[3,5], Lennert Janssen[1], Lodewyk Wessels[4], Thijn R. Brummelkamp[2], and Jacques Neefjes[1]

Abstract

The topoisomerase II poisons doxorubicin and etoposide constitute longstanding cornerstones of chemotherapy. Despite their extensive clinical use, many patients do not respond to these drugs. Using a genome-wide gene knockout approach, we identified Keap1, the SWI/SNF complex, and C9orf82 (CAAP1) as independent factors capable of driving drug resistance through diverse molecular mechanisms, all converging on the DNA double-strand break (DSB) and repair pathway. Loss of Keap1 or the SWI/SNF complex inhibits generation of DSB by attenuating expression and activity of topoisomerase IIα, respectively, whereas deletion of C9orf82 augments subsequent DSB repair. Their corresponding genes, frequently mutated or deleted in human tumors, may impact drug sensitivity, as exemplified by triple-negative breast cancer patients with diminished SWI/SNF core member expression who exhibit reduced responsiveness to chemotherapy regimens containing doxorubicin. Collectively, our work identifies genes that may predict the response of cancer patients to the broadly used topoisomerase II poisons and defines alternative pathways that could be therapeutically exploited in treatment-resistant patients. *Cancer Res; 75(19); 4176–87. ©2015 AACR.*

Introduction

Topoisomerase II (Topo II) poisons, including those of the anthracycline and podophyllotoxin families, are among the major classes of chemotherapeutics used to treat a wide spectrum of tumors. These drugs trap Topo II onto the DNA and inhibit DNA religation, hereby "poisoning" the enzyme and generating DNA double-strand breaks (DSB; ref. 1). Despite their broad applicability, resistance constitutes a frequent clinical limitation (2). Given the serious side effects associated with their administration, development of a comprehensive panel of treatment predicting factors could provide a useful clinical tool for matching chemotherapy to individual patients (1).

Anthracyclines, with doxorubicin as their prominent example, constitute an especially effective class of anticancer drugs, as they intercalate into the DNA and evict histones from the chromatin, concomitant to inhibiting Topo II after the formation of a DNA DSB (3, 4). As a result, the DNA damage response is attenuated and the epigenome becomes deregulated at defined regions in the genome (3, 5). The cellular pathways contributing to doxorubicin resistance have been interrogated extensively, and the drug transporter ABCB1 (MDR1), capable of exporting doxorubicin from cells (2), has emerged as a major player in this context. Despite its role in drug removal at the blood–brain barrier, inhibition of ABCB1 failed to satisfactorily revert unresponsiveness to doxorubicin in the clinic (6). Other factors, acting either alone or in combination with proteins such as ABCB1, have been implicated in doxorubicin resistance through the downregulation of either Topo II or other DNA damage response (DDR) pathway constituents (7, 8). Thus far, none of the above factors have been shown to individually account for the observed variability in patients' responses to doxorubicin (1, 9). Taken together, the findings reported to date suggest the existence of other as of yet undefined molecular determinants instrumental in the conversion to a doxorubicin-resistant state.

Herein we report on a genome-wide screen for factors driving resistance to doxorubicin using a knockout approach in haploid cells (10). With the aim of approximating the physiologic situation of patient drug exposure, and by extension drug resistance, in the tissue culture environment, we iteratively subjected cells to doxorubicin for three brief periods as a means of selecting for relative drug resistance. Our screening methodology yielded two previously described contributors to drug resistance: the aforementioned transporter ABCB1 (2) and the stress response gene Keap1 (11). We also identified several novel factors: the gene

[1]Division of Cell Biology, The Netherlands Cancer Institute, Amsterdam, the Netherlands. [2]Division of Biochemistry, The Netherlands Cancer Institute, Amsterdam, the Netherlands. [3]Division of Molecular Pathology, The Netherlands Cancer Institute, Amsterdam, the Netherlands. [4]Division of Molecular Carcinogenesis, The Netherlands Cancer Institute, Amsterdam, the Netherlands. [5]Division of Pathology, The Netherlands Cancer Institute, Amsterdam, the Netherlands.

Note: Supplementary data for this article are available at Cancer Research Online (http://cancerres.aacrjournals.org/).

R.H. Wijdeven and B. Pang contributed equally to this article.

Present address for B. Pang: Department of Genetics, School of Medicine, Stanford University, Stanford, CA 94305.

Corresponding Author: Jacques Neefjes, Netherlands Cancer Institute, Plesmanlaan 121, Amsterdam, 1066 CX, Netherlands. Phone: 312-0512-2017; Fax: 312-0512-2029; E-mail: j.neefjes@nki.nl

doi: 10.1158/0008-5472.CAN-15-0380

Published OnlineFirst August 10, 2015; DOI: 10.1158/0008-5472.CAN-15-0380

product of C9orf82 that appears to function as an inhibitor of DNA damage repair and the chromatin remodeling SWI/SNF complex subunits SMARCB1 and SMARCE1. Depletion of either Keap1, C9orf82, or SMARCB1 was found to induce cellular resistance to Topo II poisons, without significantly affecting sensitivity to either Topo I inhibitors or aclarubicin (Acla), an analog of doxorubicin that does not induce DNA damage (3, 5). All genes identified in the resistance screen were found to regulate Topo II-induced DNA break formation or subsequent DNA repair. In the clinic, tumors frequently harbor mutations or deletions in Keap1, C9orf82, or components of the SWI/SNF complex (12–14). These may be relevant for patient stratification to doxorubicin-based therapies, as illustrated by the correlation between expression levels of Keap1 and the SWI/SNF complex subunits and the response of triple-negative breast cancer (TNBC) patients to doxorubicin-based treatment. Our data provide a molecular basis for patient selection in the clinic with regards to the broadly used Topo II poisons in cancer therapy.

Materials and Methods

Cell culture and constructs

HAP1 and MelJuSo cells were grown in IMDM supplemented with 8% FCS. SKBR7 and HCC1937 cells were grown in RPMI with 8% FCS. HAP1 cells were generated as described in ref. 15, sequence verified during the screen, and kept under low passage afterwards. MelJuSo cells were initially described in ref. 16 and sequence verified in 2013 (3); since then identity was confirmed by staining for marker MHCII. HCC1937 cells were obtained from ATCC (www.ATCC.org), where they were validated using STR profiling, and kept under low passage after receipt. SKBR7 cells were a kind gift from Klaas de Lint (Netherlands Cancer Institute, Division of Molecular Carcinogenesis, Amsterdam, the Netherlands) and analyzed using STR profiling in 2015. Keap1 knockdown cells were generated by transduction with lentiviral vectors containing an shRNA sequence targeting Keap1. Keap1 sh1 targeted the 5′-GCGAATGATCACAGCAATGAA-3′ sequence of Keap1 and Keap1 sh2 the 5′-CGGGAGTACATCTACATGCAT-3′ sequence. Cells were maintained under puromycin (2.5 μg/mL) selection to generate stable knockdown cells. For GFP-C9orf82, the sequence of full-length C9orf82 was cloned from an Image clone (#4648932) into the mGFP-C1 vector (Clontech) using the primers 5′-CCCAAAGCTTCCATGACGGGGAAAAAGTCCTC-3′ and 5′-CCCAGGTACCCTAGGCTGGCTTTTTTATATC-3′. MelJuSo cells were transfected using effectene (Qiagen) and cells expressing GFP or GFP-C9orf82 were maintained under continuous selection with G418 (200 μg/mL).

Haploid genetic screen

The haploid genetics screen was performed as described (10). In brief, gene trap virus was produced by transfecting the gene-trap plasmid together with packaging plasmids in HEK 293T cells. Virus was harvested, concentrated, and used to infect 1×10^8 HAP1 cells. After brief passaging to allow for protein turnover, mutagenized cells were exposed to the doxorubicin regimen described below. Drug-resistant cells were expanded, genomic DNA was isolated, and subsequently retroviral insertion sites were amplified by inverse PCR and mapped by parallel sequencing (Illumina HiSeq2000) of the genomic inserts. The enrichment of insertions in the drug-treated group was calculated by comparing the number of insertions between the doxorubicin-treated group and an unselected population (15) using a one-sided Fisher exact test. These values were corrected for false discovery rate using the Benjamini and Hochberg method (10).

Generation of null alleles using CRISPR-Cas9

CRISPR targeting sequences were designed on the basis of the tool from crispr.mit.edu (17). Oligos were cloned into the pX330 backbone (18) and transfected using effectene (Qiagen) together with a vector containing a guide RNA to the zebrafish *TIA* gene (5′-ggtatgtcgggaacctctcc-3′) and a blasticidin resistance gene with a 2A sequence that is flanked by two TIA target sites. Cells positive for both vectors excise the blasticidin resistance gene from the vector and will sporadically incorporate it into the targeted genomic locus by nonhomologous end joining (NHEJ; ref. 19). Successful integration of the cassette into the targeted gene disrupts the allele and renders cells resistant to blasticidin. The targeting sequences were: SMARCB1: KO1, 5′-TGGCGCTGAGCAAGACCTTC-3′ and KO2, 5′-TGGCGCTGAGCAAGACCTTC-3′, C9orf82: KO1, 5′-CAACGCGGGTACGATGTCCG-3′ and KO2, 5′-TGACGGGGAAAAAGTCCTCC-3′, and Nrf2: 5′-TGGAGGCAAGATATAGATCT-3′. Cells were selected on blasticidin (10 μg/mL) for two days and knockout clones were validated by sequencing the genomic DNA. The following primers were used to detect deletion at the genomic level: SMARCB1 fw: 5′-CATTTCGCCTTCCGGCTTCGG-3′, SMARCB1 rv: 5′-CTCGGAGCCGATCATGTAGAACTC-3′, C9orf82 fw: 5′-GGAAGTGACGCATAACCTGCGAC-3′, C9orf82 rv: 5′-CTGCAAGGAGCCCGAGACG-3′, Nrf2 fw: 5′-GACATGGATTTGATTGACATACTTTGGAGGC-3′, Nrf2 rv: 5′-CTGACTGGATGTGCTGGGCTGG-3′.

Reagents and siRNA transfections

Doxorubicin, etoposide, and topotecan were obtained from Pharmachemie and daunorubicin was obtained from Sanofi-Aventis. Aclarubicin was obtained from Santa Cruz. Antibodies used for immunoprecipitation, Western blot and microscopy: mouse anti-Keap1, mouse anti-tubulin, mouse anti-actin (all from Sigma), rabbit anti-Topoisomerase II, rabbit anti-SMARCB1, rabbit anti-SmarcA4, rabbit anti-SMARCE1, rabbit anti-ARID1a (all from Bethyl laboratories), mouse anti-γH2AX, rabbit anti-H2A (Millipore).

For siRNA-mediated depletion of SMARCA4 and SMARCB1, cells were reverse transfected with DharmaFECT transfection reagent #1 and 50 nmol/L siRNA (Human siGenome SMARTpool; Dharmacon) according to the manufacturing protocol. Briefly, siRNAs and DharmaFECT were mixed and incubated for 20 minutes, after which cells were added and left to adhere. Three days later, cells were treated and lysed for SDS-PAGE and Western blotting analysis or left to grow out for three more days for the cell viability assay.

Long-term proliferation assays

Cells were seeded into 12-well plates (5,000 cells per well). The next day, drugs were added at concentrations indicated and cultured for 2 hours. Subsequently, drugs were removed and cells were left to grow for 7 to 9 days, fixed using 3.7% formaldehyde, and stained using 0.1% Crystal violet solution (Sigma). Quantification of colonies was done by ImageJ.

Short-term growth inhibition assays

Cells were seeded into 96-well plates (2,000 cells per well) and exposed the next day to the indicated drugs (for siRNA

Published OnlineFirst August 10, 2015; DOI: 10.1158/0008-5472.CAN-15-0380

knockdowns, cells were seeded three days before treatment). Drugs were removed two hours later and cultured for an additional 72 hours. Cell viability was measured using the Cell Titer Blue viability assay (Promega). Relative survival was normalized to the untreated control and corrected for background signal.

Coimmunoprecipitation and Western blotting

For coimmunoprecipitation experiments of nuclear proteins, cells were trypsinized, counted and lysed (25 mmol/L HEPES pH 7.6, 5 mmol/L $MgCl_2$, 25 mmol/L KCl, 0.05 mmol/L EDTA, 10% glycerol and 0.1% NP-40 supplemented with complete EDTA-free Protease Inhibitor Cocktail (Roche)). Nuclei were isolated by spinning at 1,300 × *g* and subsequently sonicated for 30 minutes in lysis buffer [50 mmol/L Tris-HCl, pH 8.0, 150 mmol/L NaCl, 0.1% NP-40 supplemented with Protease Inhibitor Cocktail (Roche)]. Chromatin was removed by centrifugation (5 minutes at 12,000 × *g*) and the supernatant was precleared with protein G dynabeads (Life Technologies). Lysate was incubated overnight with 3 μg antibody and 20 μL protein G Dynabeads. Beads were washed extensively and resuspended in SDS-sample buffer (2% SDS, 10% glycerol, 5% β-mercaptoethanol, 60 mmol/L Tris-HCl pH 6.8 and 0.01% bromophenol blue) before analysis by SDS-PAGE.

For whole-cell lysate analyses, cells were lysed directly in SDS sample buffer (2% SDS, 10% glycerol, 5% β-mercaptoethanol, 60 mmol/L Tris-HCl pH 6.8 and 0.01% bromophenol blue). Samples were analyzed by SDS-PAGE and Western blotting. Blocking of the filter and antibody incubations were done in PBS supplemented with 0.1 (v/v)% Tween and 5% (w/v) bovine milk powder.

Constant-field gel electrophoresis

DNA DSBs were quantified by constant-field gel electrophoresis as described (20). In short, HAP1 cells were treated with doxorubicin or Etoposide for 2 hours. Drugs were removed and cells were lysed and processed immediately to isolate the DNA. Samples were separated on a 0.8% agarose gel to separate faster migrating broken DNA from intact DNA and fragments of over >1 MB. Images were analyzed by ImageJ.

Flow cytometry

Cells were treated with doxorubicin (2 μmol/L) for one hour and trypsinized and fixed with 3.7% formaldehyde. Fluorescence of doxorubicin was measured directly using a FACSCalibur flow cytometer (BD Biosciences) and further analyzed by FlowJo software.

cDNA synthesis and qPCR

RNA isolation, cDNA synthesis, and quantitative RT-PCR were performed as described previously (21). The primers for detection of Keap1, NQO1, and GAPDH expression were: Keap1 fw: 5′-CTGGAGGATCATACCAAGCAGG-3′, Keap1 rv: 5′-GAACATGGCCTTGAAGACAGG-3′, NQO1 fw: 5′-GGGCAAGTCCATCCCAACTG-3′, NQO1 rv: 5′-GCAAGTCAGGGAAGCCTGGA-3′, GAPDH fw: 5′-TGTTGCCATCAATGACCCCTT-3′, GAPDH rv: 5′-CTCCACGACGTACTCAGCG-3′.

Confocal microscopy

MelJuSo cells were seeded on coverslips and treated as indicated in the respective experiments. Cells were fixed in 3.7% formaldehyde for 10 minutes and permeabilized by 0.1% Triton X-100. Staining was performed with the antibodies mentioned above or with phalloidin (Invitrogen) to stain F-actin and DAPI (Invitrogen) to stain DNA. Images were acquired using a Leica TCS SP5 confocal microscope.

Chromatin association assay

HAP1 cells were seeded and treated with Etoposide for 15 minutes before lysis when indicated. Cells were lysed in lysis buffer (25 mmol/L HEPES pH 7.6, 5 mmol/L $MgCl_2$, 25 mmol/L KCl, 0.05 mmol/L EDTA, 10% glycerol, 0.1% NP-40) and nuclei were spun down and resuspended at a concentration of 60 million/mL in buffer (20 mmol/L Tris-HCl pH 7.6, 3 mmol/L EDTA). Twenty-five microliter samples were adjusted to the indicated NaCl concentrations to a total volume of 50 μL. After mixing and incubation on ice for 20 minutes, chromatin was spun down and resuspended in sample buffer. After sonication, samples were analyzed by SDS-PAGE and Western blotting.

Gene expression analysis of the neoadjuvant breast cancer cohort

Gene expression data was obtained from 113 pretreatment biopsies of TNBC patients treated at the Antoni van Leeuwenhoek hospital (associated to the NKI) and scheduled to receive neoadjuvant chemotherapy. All patients had a breast carcinoma with either a primary tumor size of at least 3 cm, or the presence of axillary lymph node metastases. A treatment regimen was assigned to each patient, consisting of six courses of dose-dense doxorubicin/cyclophosphamide (ddAC). If the therapy response was considered unfavorable by MRI evaluation after three courses, ddAC was changed to capecitabine/docetaxel (XD). Response to therapy was defined as pathological complete response (pCR) or no pathologic complete response at the time of surgery.

Sixty-three Samples were labeled and hybridized to Illumina 6v3 arrays (Illumina). Data were log2 transformed and between-array normalized using simple scaling. When a single gene was represented by multiple probes, the probe with the highest variance was chosen. The data is made available through the GEO database, accession GSE34138 (http://www.ncbi.nlm.nih.gov/geo/query/acc.cgi?acc=GSE34138; ref. 22). Fifty samples were profiled using RNAseq. Strand-specific sequencing libraries were generated using the TruSeq Stranded mRNA sample preparation guide (Illumina Part # 15031047 Rev. E) according to the manufacturer's instructions. Deep Sequencing was done with a HiSeq2000 machine (Illumina Inc). The reads are mapped against the human reference (hg19) using Tophat (version 2.0.6) (23). Tophat was supplied with a known set of genemodels using a GTF file (Ensembl version 66). HTSeq-count (24) was used to define gene expressions. This tool generates a list of the total number of uniquely mapped reads for each gene that was provided in the GTF. These data were normalized on the basis of the relative library size using the DESeq2 R package (25) and subsequently log transformed.

Statistical analysis

All experiments were performed at least three times in an independent manner. All data are presented as means ± SD. The results were analyzed by using a paired two-tailed Student *t* test

Published OnlineFirst August 10, 2015; DOI: 10.1158/0008-5472.CAN-15-0380

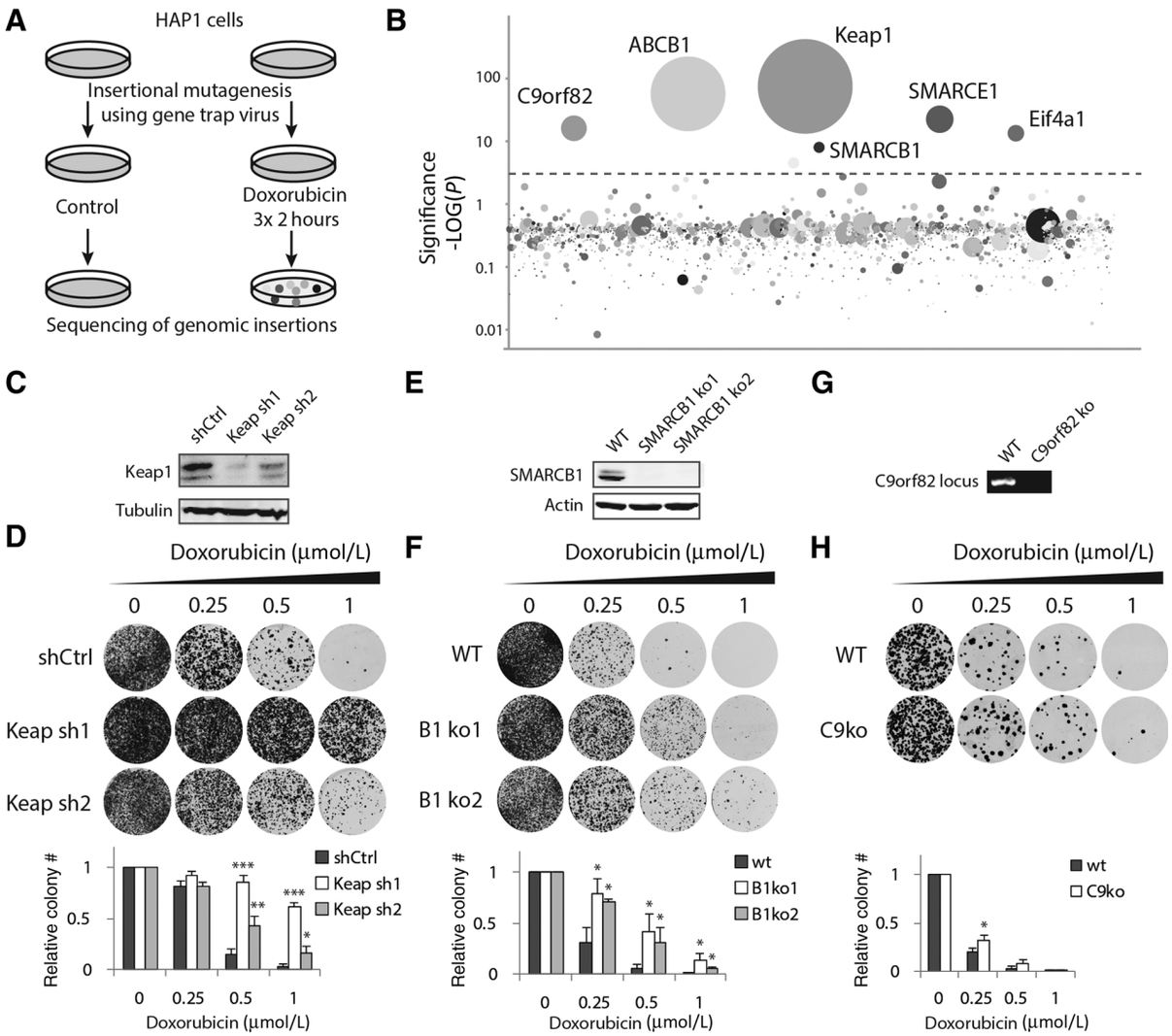

Figure 1.
Genome-wide mutagenesis screen identifies Keap1, the SWI/SNF complex, and C9orf82 as regulators of doxorubicin resistance. A, schematic set-up of the haploid genetics screen to identify genes involved in doxoruibicin (Doxo) resistance. B, screening results. The *y* axis indicates the significance of enrichment of gene-trap insertions in doxorubicin-treated compared with nontreated control cells. The circles represent genes and their size corresponds to the number of independent insertions mapped in the gene. For more hits, see Supplementary Table S1. C, Keap1 silencing was determined by Western blotting analysis. D, long-term colony formation assay with HAP1 cells transduced with shRNAs targeting Keap1 or a control shRNA. Cells were treated with the indicated concentration doxorubicin for 2 hours and left to grow out. After 9 days, cells were fixed, stained, and imaged. Quantification of colony numbers per plate and condition from three independent experiments (+SD) are shown below the images. E, Western blotting showing depletion of SmarcB1 by two independent CRISPR-targeting sequences. F, long-term colony formation assays for wild-type and SMARCB1-depleted cells. Results from three independent experiments (+SD) were quantified and are shown below the images. G, genomic PCR showing the knockout of C9orf82. H, long-term colony formation assay for wild-type and C9orf82-depleted cells. Results from three independent experiments (+SD) were quantified and are shown below the images. Statistical significance was calculated compared to control (*, $P < 0.05$; **, $P < 0.01$; ***, $P < 0.001$).

(unpaired for the data in Fig. 6B). Significance was calculated using Microsoft Excel and defined as $P < 0.05$.

Results

Identification and validation of doxorubicin-resistance factors Keap1, C9orf82, and the SWI/SNF complex

To identify genetic determinants involved in resistance to doxorubicin, we performed a genome-wide insertional mutagenesis screen in haploid cells using a gene trap retrovirus (10). A genomic insertion of the virus into the sense direction of a gene disrupts its expression and often results in a complete knockout of the gene. HAP1 cells were infected with a gene trap retrovirus to generate a pool of randomly mutagenized cells and briefly passaged prior to drug exposure. To recapitulate the normal pharmacokinetics of doxorubicin in a tissue culture setting, we exposed these cells for 2 hours to 1 μmol/L doxorubicin, which is within the peak plasma dose of standard treatment of cancer patients (26). Cells were treated weekly for 3 weeks, after which surviving cells were grown out and insertions were mapped and

Published OnlineFirst August 10, 2015; DOI: 10.1158/0008-5472.CAN-15-0380

aligned to the human genome (Fig. 1A). Disruptions of six genes were significantly enriched ($P < 0.00005$) in the surviving population compared with the untreated control (Fig. 1B; Supplementary Table S1) Among these were two previously reported factors, *ABCB1* (6) and *Keap1* (27), as well as novel factors, including the SWI/SNF subunits, *SMARCB1* and *SMARCE1*, the *C9orf82* gene, and the translation initiation factor *Eif4a1*. Canonical doxorubicin target Topo IIα appeared just below the threshold, with an adjusted *P* value of 0.01. ABCB1 contained mostly antisense mutations following selection, which could enhance its expression (unpublished observation). All other enriched genes contained at least five independent insertions in the sense direction, leading to their inactivation. Identification of *Keap1* provided validation of the screening methodology, as it has already been associated with resistance to several anticancer drugs, including doxorubicin (11, 12, 28).

To validate the screen hits, we generated HAP1 cells stably expressing either control shRNA or two independent shRNAs targeting Keap1, which reduced Keap1 expression by 50% to 80% (Fig. 1C and Supplementary Fig. S1A). These knockdown cell lines were subsequently exposed to doxorubicin for 2 hours, followed by drug wash out and outgrowth. As expected, Keap1 depletion conferred doxorubicin resistance as illustrated in both colony formation and viability assays (Fig. 1D and Supplementary Fig. S1B).

We then proceeded to validate the novel screen hits. Two independent CRISPR/Cas9 constructs targeting the *SMARCB1* gene (Fig. 1E) rendered the cells more resistant to doxorubicin, both in colony formation and viability assays (Fig. 1F and Supplementary Fig. S1C). Independent identification of two members of the SWI/SNF chromatin-remodeling complex (29), SMARCB1, and SMARCE1, suggested that deregulation of the complex as a whole may drive resistance to doxorubicin. Although we could not validate a role for SMARCE1 in resistance to doxorubicin, shRNA-mediated depletion of the SWI/SNF core members SMARCA4 and ARID1A, alongside SMARCB1, induced resistance to doxorubicin (Supplementary Fig. S1D and S1E), supporting the notion that loss of the SWI/SNF complex functionality confers resistance to doxorubicin.

While we did not further pursue the translational elongation complex subunit Eif4a1, we tested the contribution of the open reading frame 82 on chromosome 9 (C9orf82) to doxorubicin sensitivity. A small but significant growth advantage was observed in response to doxorubicin treatment in C9orf82 knockout cells using a colony formation assay (Fig. 1G and H). Collectively, our genome-wide screen identified multiple novel factors capable of incurring resistance to doxorubicin in a cell culture setting.

Cross-resistance to other DNA-damaging drugs

Doxorubicin is known to act on cells by a combination of Topo II poisoning, eviction of histones from the chromatin and the generation of reactive oxygen species (ROS; refs. 3, 4, 30). To establish which of these mechanisms are affected by Keap1, the SWI/SNF complex, and C9orf82, we treated the respective knockdown or knockout cell lines with either the different Topo II poisons daunorubicin (an anthracycline with a structure and activity similar to doxorubicin) or etoposide (a Topo II poison structurally unrelated to doxorubicin and incapable of evicting histones), or with aclarubicin (an anthracycline family member that evicts histones, induces ROS and inhibits Topo II but does not induce DNA damage; ref. 31). Silencing Keap1 or eliminating SMARCB1 or C9orf82 rendered cells more resistant to both etoposide and daunorubicin, but not aclarubicin (Fig. 2A–C) as indicated by viability as well as colony formation assays. Given the properties of the three drugs, these observations provide hints as to the molecular mechanisms underlying doxorubicin resistance via these genes, through the DNA damage arm. Interestingly, C9orf82 depletion rendered cells more resistant to etoposide than to doxorubicin or daunorubicin, suggesting that fast DNA repair may be critical for this gene's mode of action, as doxorubicin and daunorubicin attenuate DNA repair by eviction of H2AX (5).

Importantly, depletion of none of our hits induced measurable resistance to the topoisomerase I poison topotecan that induces single-strand DNA breaks (Fig. 2C and D), suggesting that Keap1, the SWI/SNF complex, and C9orf82 are involved in the Topo II-dependent DDR pathway.

Keap1 controls the expression of Topo IIα independently of Nrf2

Of the three validated resistance factors from the screen, Keap1 has been previously linked to chemoresistance (11, 27, 32). Keap1 functions as an E3 ligase adaptor and is known to mediate the degradation of Nrf2, a transcription factor for oxidative stress response genes (33). Upregulation of Nrf2 desensitizes cells to several anticancer drugs, including alkylating and antimitotic agents, which suggests that downregulation of Keap1 may induce drug resistance by stabilizing Nrf2 (12, 27, 28). To test this, we used CRISPR/Cas9 technology to generate Nrf2 knockout cells (Fig. 3A), functionally validated by a drastic reduction of expression of Nrf2 target gene *NQO1* (Supplementary Fig. S2A). Unexpectedly, silencing of Keap1 in the Nrf2-null background still endowed cells more resistance to doxorubicin and etoposide (Fig. 3A), implying the existence of an Nrf2-independent mechanism for Keap1 in modulating cellular responsiveness to Topo II–dependent DNA damage inducers.

Double-strand DNA break analysis indicated that loss of Keap1 significantly decreases the amount of such breaks induced by either etoposide or doxorubicin treatment (Fig. 3B). These results were corroborated by the observed reduction in the DDR as measured by γ-H2AX following exposure to etoposide (doxorubicin evicts H2AX from the DNA and was therefore not used to measure the DDR after drug exposure; Fig. 3C). Keap1 silencing did not affect uptake of doxorubicin (monitored by intrinsic fluorescence of the drug by flow cytometry, Fig. 3D), suggesting that Keap1 may control either the levels or activity of the drug target, Topo IIα. Cells depleted of Keap1 had lower Topo IIα expression levels relative to the control (Fig. 3E), which was independent of Nrf2 activity (Fig. 3F). A link between Topo IIα expression levels and resistance against Topo II poisons has been previously suggested (7, 34, 35). These observations indicate that Keap1 can control resistance to Topo II poisons by two distinct mechanisms, regulating Nrf2 expression to control a series of stress-response genes and by mediating the expression of the canonical target Topo IIα.

C9orf82 regulates repair of DNA damage induced by TopoII poisons

In contrast with the previously studied role of Keap1 in drug resistance, the role of C9orf82 in this context has not been addressed, with its only function thus far assigned being negative regulation of apoptosis (36). We began by addressing the effect of this gene on Topo II induced DSB formation and repair as pertaining to Topo II function. Monitoring the DNA DSBs and

Published OnlineFirst August 10, 2015; DOI: 10.1158/0008-5472.CAN-15-0380

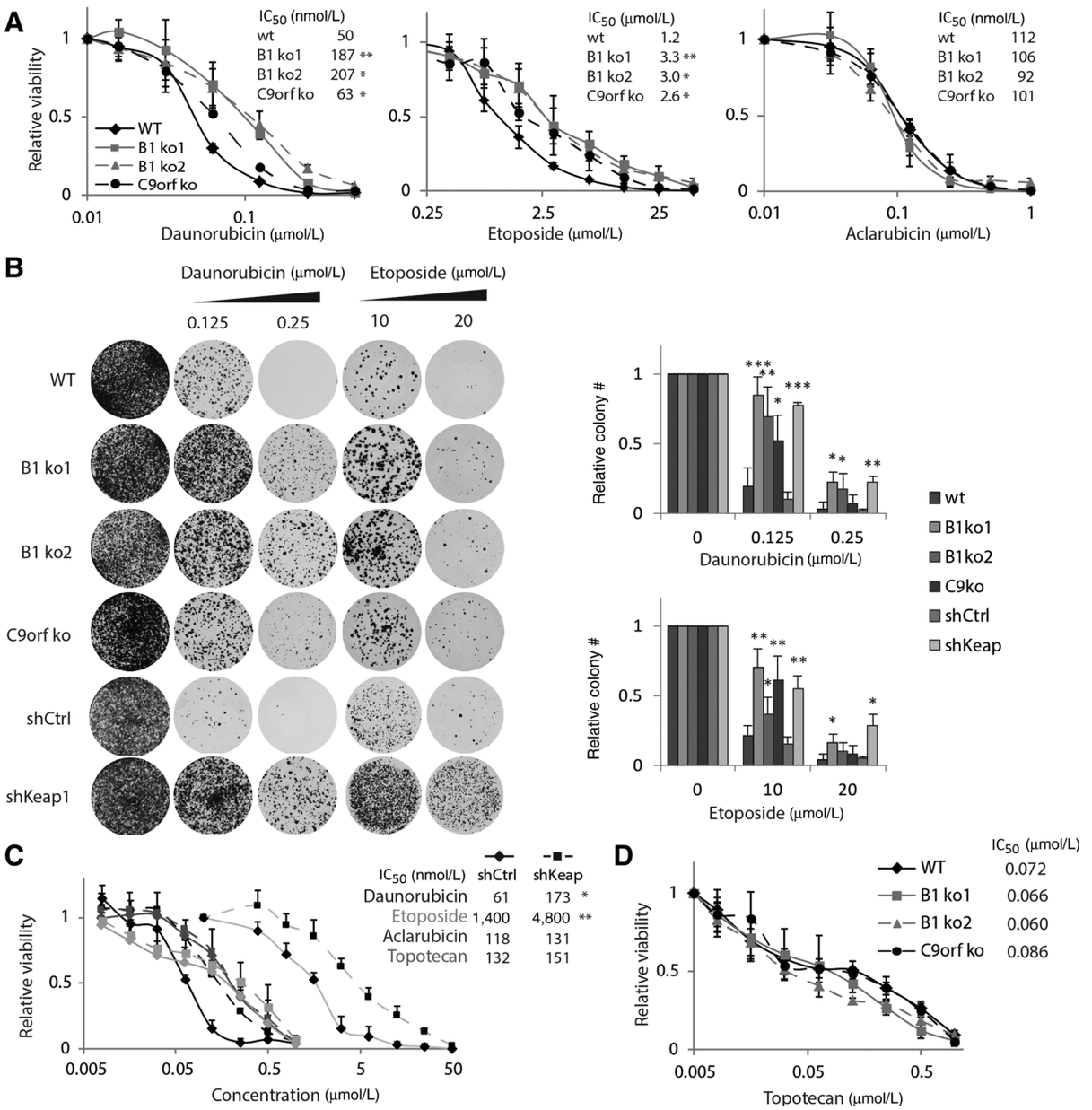

Figure 2.
Keap1, SWI/SNF, and C9orf82 control sensitivity to Topo II but not Topo I inhibition or aclarubicin. A, HAP1 cells depleted for SMARCB1 or C9orf82 were treated for 2 hours with daunorubicin, etoposide, or aclarubicin and cell viability was analyzed 72 hours later by a CellTiter Blue assay. B, long-term colony formation assay with HAP1 cells depleted for SMARCB1, C9orf82, or Keap1 that were treated for 2 hours with the indicated drug at different concentrations. C, HAP1 cells stably expressing shCtrl or shKeap1 were treated for 2 hours with daunorubicin, etoposide, aclarubicin, or topotecan and cell viability was analyzed 72 hours later by a CellTiter Blue assay. D, HAP1 cells depleted for SMARCB1 or C9orf82 were treated for 2 hours with topotecan and cell viability was analyzed 72 hours later by a CellTiter Blue assay. All experiments shown are representatives of at least three independent experiments. Statistical significance was calculated as compared with control cells (*, $P < 0.05$; **, $P < 0.01$; ***, $P < 0.001$).

the resulting DNA damage response following exposure to either doxorubicin or etoposide revealed no difference in the initial levels of DNA damage incurred between the control and C9orf82 knockout cells (Fig. 4A and B). Strikingly, the resolution of the DNA damage response signal following etoposide treatment (as visualized by γ-H2AX) was significantly accelerated in C9orf82 knockout cells (Fig. 4B). Similar results were obtained with another independently generated C9orf82 knockout clone (Supplementary Fig. S3A–S3C). Conversely, ectopic expression of GFP-tagged C9orf82 in MelJuSo melanoma cells (a cell line with fast DNA repair kinetics) led to a stronger and more persistent γ-H2AX DNA damage response upon etoposide treatment (Fig. 4C). As DNA repair already takes place during the first hour of etoposide treatment, these data indicate that C9orf82

Published OnlineFirst August 10, 2015; DOI: 10.1158/0008-5472.CAN-15-0380

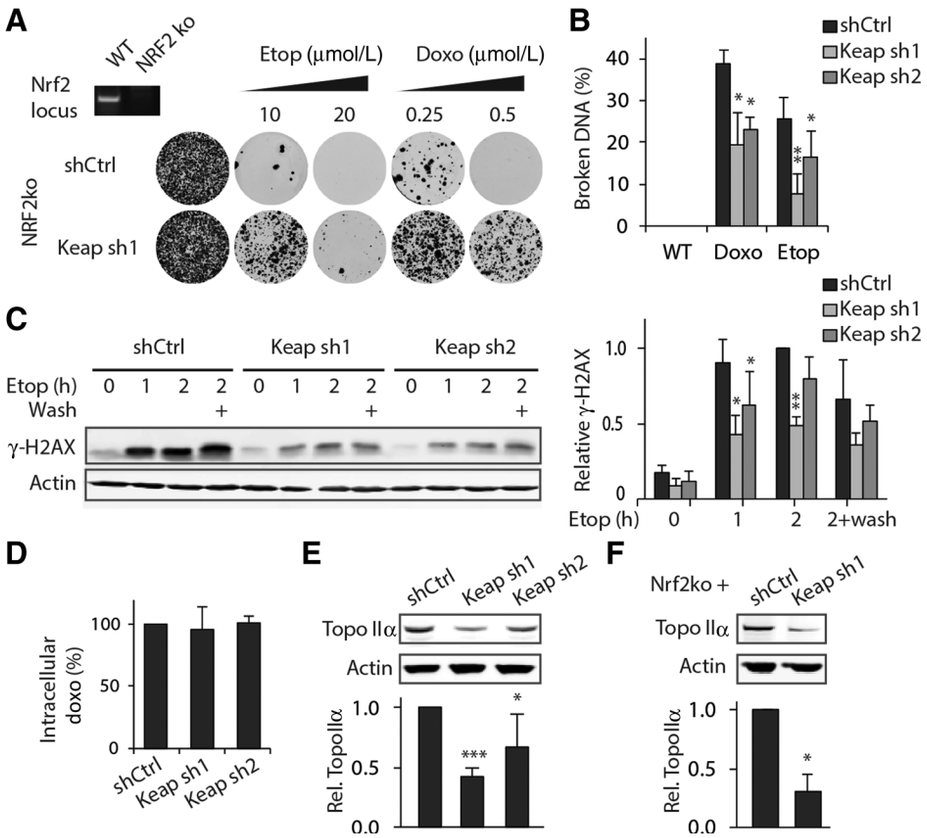

Figure 3.

Keap1 controls Topo IIα expression independently of Nrf2. A, long-term colony growth assay for HAP1 cells depleted for Nrf2 and further stably transduced with shKeap1 or shCtrl. Cells were treated for 2 hours with doxorubicin (Doxo) or etoposide (Etop) at the indicated concentrations and left to grow out for 9 days. Inset, the DNA gel shows loss of the genomic Nrf2 locus in the knockout cells. B, analysis of the amount of etoposide- or doxorubicin-induced DNA breaks using constant field gel electrophoresis. HAP1 cells were treated for 2 hours with 1 μmol/L etoposide or doxorubicin, lysed, and analyzed. Shown is the quantification of the broken DNA relative to input. C, Hap1 cells were treated with 5 μmol/L etoposide for the indicated time points, or the drug was washed out after 2 hours and cells were left to recover for another 2 hours (lanes "+"), lysed, and analyzed by SDS-PAGE and Western blotting. Right, quantification of the γ-H2AX signal normalized to actin. The signal of wild-type cells treated for 2 hours was set at 1. D, cells were treated with 2 μmol/L doxorubicin for 1 hour and doxorubicin levels were analyzed using flow cytometry. Control shRNA was set at 1. E, Western blotting analysis for expression of Topo IIα in HAP1 cells silenced for Keap1. For quantification, the signal was normalized to actin and the shCtrl was set at 1. F, Western blotting analysis for expression of Topo IIα in HAP1 Nrf2ko cells stably depleted or not for Keap1. All results are mean ± SD of biologic triplicates, except for E, which are biologic quadruplicates. Statistical significance was calculated compared to control (*, $P < 0.05$; **, $P < 0.01$; ***, $P < 0.001$).

influences the kinetics of γ-H2AX resolution and hereby the DNA damage response. To assess whether C9orf82 regulates DSB repair itself, we determined the DSB repair kinetics in cells overexpressing either GFP or GFP-C9orf82 (Fig. 4D), with the latter resulting in decreased etoposide-induced DNA DSB repair. This suggests that C9orf82 decreases the rate of DNA repair.

Although C9orf82 localizes primarily in the nucleus (Fig. 4E), it is unlikely to directly inhibit DNA repair, as it is not recruited to Etop-induced γ-H2AX foci (Supplementary Fig. S3D). On this basis, C9orf82 appears to attenuate DNA DSB repair induced by Topo II poisons, for its loss serves to accelerate DNA damage repair, thereby promoting resistance to DNA DSB inducers such as doxorubicin and etoposide. The exact molecular mechanism of DNA repair modulation by this novel protein is at present unclear.

The SWI/SNF complex controls chromatin loading of Topo II to confer drug resistance

In addition to the resistance factors described above, we also identified two subunits of the SWI/SNF complex involved in the resistance to Topo II poisons. The SWI/SNF complex is known to modulate transcription through chromatin remodeling (29). In addition, it has recently been shown to mediate decatenation of chromatids during mitosis by loading Topo IIα onto the DNA (37). The latter suggests a possible means by which the SWI/SNF complex may affect the susceptibility of cells to Topo II poisons, by reducing the chromatin loading and activity of Topo IIα. To address this, HAP1 cells either proficient in or depleted of the SWI/SNF subunit SMARCB1 were exposed to etoposide or doxorubicin, and the resulting DNA DSBs were quantified. The SMARCB1-depleted cells exhibited significantly lower levels of such DNA breaks (Fig. 5A), as well as reduced DNA damage response signaling, as visualized by γ-H2AX analysis (Fig. 5B and C). These changes were not a result of drug uptake deficiency (Fig. 5D) or altered expression levels of Topo IIα (Fig. 5E). Given that SMARCB1 interacts with Topo IIα (Fig. 5F; ref. 37), the expected reduction in loading of Topo IIα onto the DNA in cells compromised for SMARCB1 presents a likely explanation for the diminished efficacy of

Published OnlineFirst August 10, 2015; DOI: 10.1158/0008-5472.CAN-15-0380

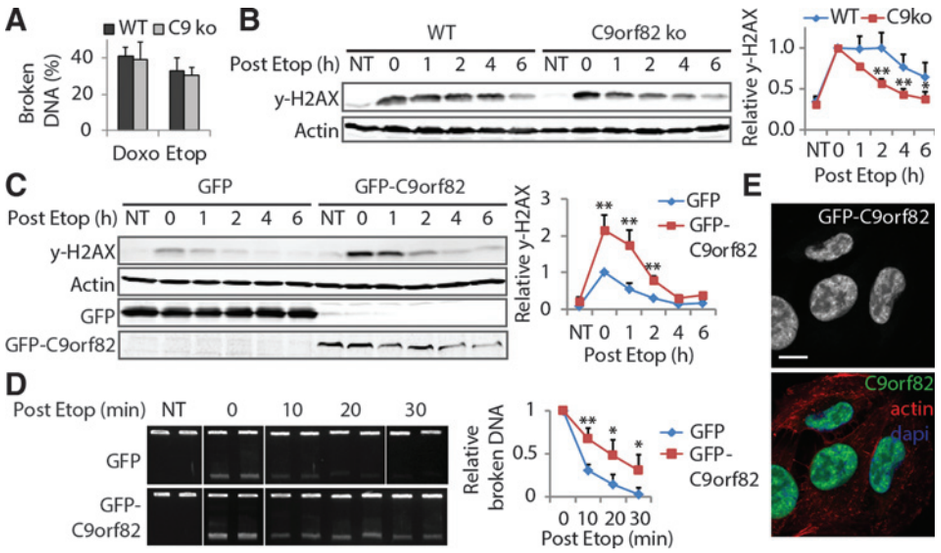

Figure 4.

C9orf82 regulates DNA double-strand break repair. A, analysis of the amount of etoposide- or doxorubicin-induced DNA breaks using constant field gel electrophoresis. HAP1 cells were treated for 2 hours with 1 μmol/L etoposide (Etop) or doxorubicin (Doxo), lysed, and analyzed. Shown is the quantification of broken DNA relative to input. B, Western blotting analysis for γ-H2AX. Cells were treated with 1 μmol/L etoposide for 1 hour, washed, and lysed at the indicated time points. Right, quantification of the signals detected on the Western blot analysis. Signals were normalized to actin and t = 0 was set at 1. C, GFP or GFP-C9orf82 overexpressing MelJuSo cells were exposed to 5 μmol/L etoposide and analyzed for γ-H2AX as in B. D, MelJuSo cells stably overexpressing GFP or GFP-C9orf82 were treated with 1 μmol/L etoposide for 2 hours. Drugs were removed before further culture. Cells were lysed at the indicated time points post drug removal. DNA break repair was analyzed using constant field gel electrophoresis. Lower band represents the broken DNA and the top band the intact DNA. Separate panels are different cut-outs from the same gel. For quantification, t = 0 of the GFP or GFP-C9orf82 cells was set at 1. E, cellular localization of C9orf82 by confocal imaging of MelJuSo cells stably expressing GFP-C9orf82 and stained for DAPI (blue) and actin (red). Scale bar, 10 μm. All experiments shown are mean + SD of three independent experiments. Statistical significance compared with control (*, $P < 0.05$; **, $P < 0.01$). NT, nontreated.

Topo II poisons in these cells. To confirm this, we assessed the association of Topo IIα to the chromatin using a chromatin binding assay as described in ref. 37. Treatment of cells with etoposide yielded more Topo IIα loaded onto chromatin (Fig. 4G), indicating this assay can be used to assess Topo IIα activity and arrest. In line with our hypothesis, SMARCB1 depletion resulted in a decreased amount of Topo IIα loaded onto chromatin after etoposide exposure (Fig. 4G), indicating that loss of SMARCB1 reduces the level of Topo IIα that is poisoned on the chromatin. These results suggest that the SWI/SNF complex modulates resistance to TopoII poisons by controlling the loading of Topo IIα onto the DNA.

Expression of SWI/SNF subunits in epithelioid sarcoma and TNBCs correlates to doxorubicin response

Although mutations in the SWI/SNF members are frequently observed in human tumors (14), their relationship to clinical outcome is lacking. Epithelioid sarcomas are known to harbor deletions of the *SMARCB1* gene in 60% to 90% of the cases (38, 39) and are commonly treated with doxorubicin-containing regimens. Re-analysis of a previously reported dataset (39) revealed that patients with a deletion for SMARCB1 experienced more relapses after treatment (Fig. 6A), suggesting a relationship between SMARCB1 expression and treatment outcome. To further assess whether SWI/SNF status correlates directly with patient responses to treatment with Topo II poisons, we used an expression dataset of 113 human TNBC patients treated at our cancer center with a regimen of doxorubicin and cyclophosphamide. We compared the expression of the SWI/SNF complex subunits SMARCB1, SMARCA4, SMARCE1, and ARID1a with the clinical response to this treatment. Our analysis showed that patients with a pathologic complete response had a significantly higher expression of SMARCB1 and SMARCA4 (Fig. 6B), but not ARID1a or SMARCE1 (Supplementary Fig. S4A). Furthermore, by analyzing the other genes identified from the screen, we found a significant correlation between response and expression for Keap1, but not C9orf82 (Supplementary Fig. S4A). These data suggest that in TNBC patients, low expression of SMARCB1 and SMARCA4 is associated with poor response to a doxorubicin-containing regimen.

To validate that SMARCB1 and SMARCA4 causally regulate sensitivity to doxorubicin in TNBC settings, we silenced both genes in two TNBC cell lines, HCC1937 and SKBR7 (Keap1 silencing was toxic for these cells and could not be tested). Silencing of both genes rendered cells more resistant to doxorubicin (Fig. 6C) and led to a reduced induction of DNA damage signaling (Fig. 6D).

Thus, loss or reduced expression of SMARCB1 and SMARCA4 negatively affects doxorubicin-induced DNA DSB formation and leads to drug resistance in TNBC cell lines and patients.

Discussion

Annually, nearly 1 million cancer patients are treated with Topo II poisons such as doxorubicin, daunorubicin, or etoposide. Yet, resistance to these drugs persists as a major complication in cancer treatment. Because the molecular basis for this resistance is not fully understood, many patients receive ineffective treatments accompanied by adverse side effects in the absence of the corresponding clinical benefit (1). To facilitate treatment outcome

Published OnlineFirst August 10, 2015; DOI: 10.1158/0008-5472.CAN-15-0380

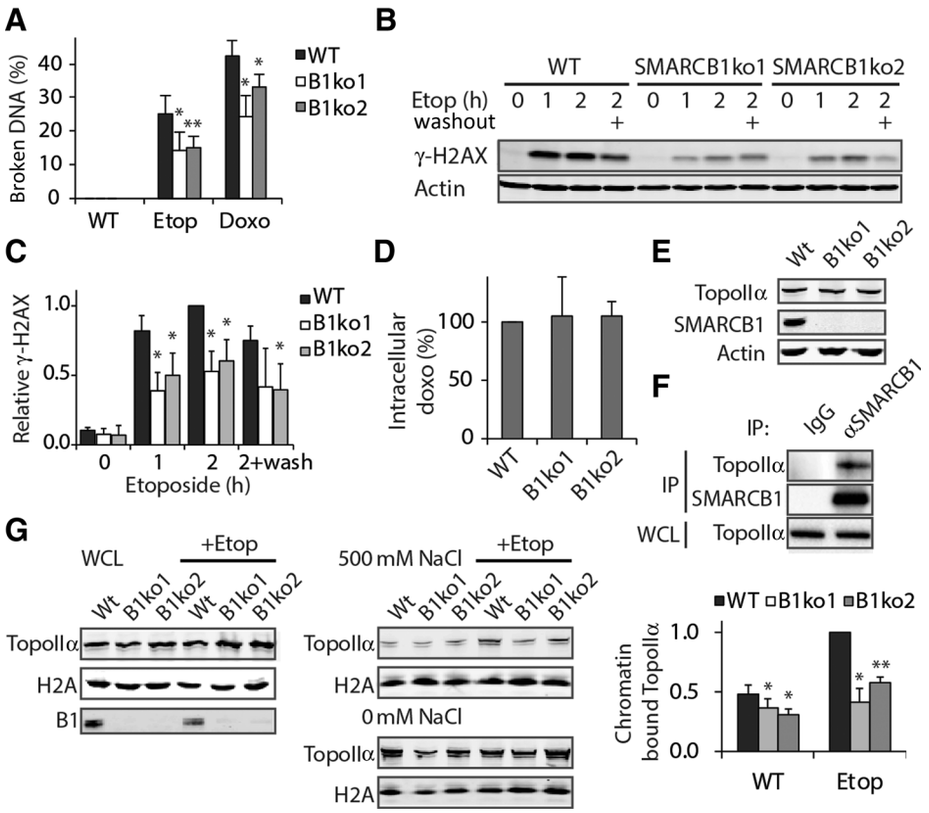

Figure 5.

The SWI/SNF complex regulates Topo IIα chromatin loading and activity. A, the amount of etoposide (Etop)- or doxorubicin (Doxo)-induced DNA breaks was quantified by constant field gel electrophoresis. HAP1 WT and SMARCB1 knockout cells were treated for 2 hours with 1 μmol/L etoposide or doxorubicin. Shown is the quantification of the relative amount of broken DNA. B, Western blot analysis for γ-H2AX after exposing cells to 5 μmol/L etopoide for the indicated time points, or first treated for 2 hours and lysed 2 hours (lanes "+") after etoposide removal. Actin is probed as a loading control. C, quantification of B. The γ-H2AX signal was normalized to the actin signal and t = 2 hours for WT was set at 1. D, quantification of doxorubicin uptake levels by flow cytometry. The different cells were incubated for 1 hour with 2 μmol/L doxorubicin before analysis. E, Western blot analysis of Topo IIα expression levels in HAP1 cells either or not depleted for SMARCB1, as indicated. Actin is shown as loading control. F, coimmunoprecipitation (IP) of SMARCB1 and Topo IIin HAP1 cells followed by SDS-PAGE and Western blotting. IgG IP was used as control. WCL, Topo II in total lysates are shown as loading control. G, chromatin association assay for Topo IIα. Chromatin pellets of indicated HAP1 cells untreated or treated with 1 μmol/L etoposide for 15 minutes were lysed directly (WCL) or treated with the indicated salt concentration (0 mmol/L or 500 mmol/L) before lysis. For quantification, the 500 mmol/L NaCl Topo IIα signal was corrected for loading (H2A) and WCL input signal. WT etoposide 15 minutes was set at 1. All experiments shown are mean + SD of independent triplicates. Statistical significance was calculated compared with control (*, $P < 0.05$; **, $P < 0.01$).

predictions for doxorubicin relative to other available alternative drugs, improved insights into the mechanisms of drug resistance are necessary. Using a genome-wide screening approach, we identified and characterized several novel factors involved in resistance to Topo II poisons. In addition to the previously described factors, including the drug transporter ABCB1 and adaptor Keap1, we identified C9orf82 and the SWI/SNF complex as novel regulators of doxorubicin resistance. Keap1, C9orf82, and SWI/SNF can all be placed in the pathway involving Topo II-induced DNA double-strand break formation and the subsequent DDR (Fig. 7). Consequently, depletion of these genes does not confer resistance to either the Topo I inhibitor topotecan, or aclarubicin, an anthracycline that does not induce DNA DSBs (3).

Keap1 has already been studied in the context of chemosensitivity to several classes of anticancer drugs, including alkylating agents, antimitotic agents, and Topo II poisons (11, 28, 32). Inhibition of its cognate substrate Nrf2 sensitizes cells to a number of these drugs, suggesting that Keap1 influences sensitivity by virtue of Nrf2 destabilization (11, 28). However, Keap1 controls several other signaling pathways (40–42), and could thus affect drug resistance in other ways. We interrogated these two options by depleting Nrf2 and found that asides from regulating Nrf2, Keap1 induces resistance to Topo II poisons by controlling the expression levels of Topo IIα. Clinically, we show that the expression of Keap1 is correlated to the response of TNBC patients to doxorubicin and cyclophosphamide. Keap1-inactivating mutations and deletions are frequently observed in human tumors (43, 44). For example, 12% to 15% of lung tumors have inactivated Keap1 (43) and as these tumors are frequently treated with combinations of etoposide and cisplatin, it may be beneficial to determine patients' Keap1 mutational status to assess the proper treatment protocol.

We also defined C9orf82 as a novel factor involved in resistance to Topo II poisons, most notably etoposide. A previous study has identified C9orf82 as a negative regulator of caspase-mediated apoptosis (36), which is not in line with our observations that

Published OnlineFirst August 10, 2015; DOI: 10.1158/0008-5472.CAN-15-0380

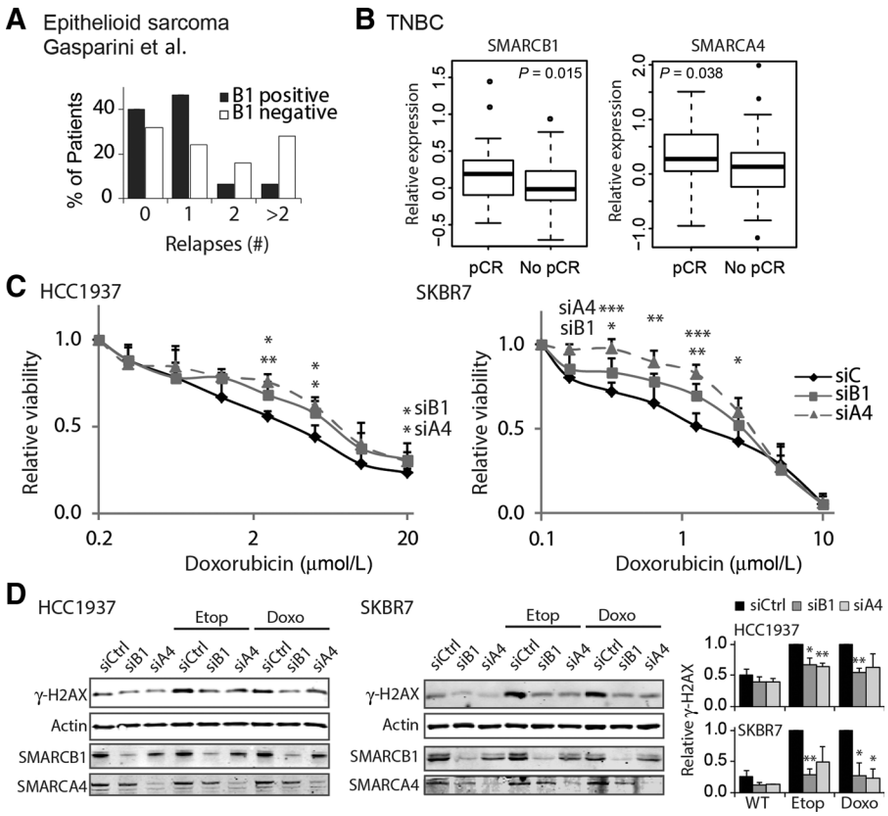

Figure 6.
SMARCB1 and SMARCA4 expression correlates to responses to doxorubicin (Doxo) in TNBC cells and patients. A, re-analysis of the number of relapses in 25 SMARCB1-negative and 15 SMARCB1-positive epithelioid sarcoma patients, as described in ref. 39. B, box plot representing the expression of SMARCB1 and SMARCA4 in 113 TNBC patients with a pathologic complete response (pCR, 46 patients) or not (no pCR, 67 patients) following a doxorubicin-containing regimen. Statistical significance was calculated using a Student *t* test. C, HCC1937 or SKBR7 cells were transfected with control siRNAs or siRNAs targeting SMARCB1 or SMARCA4. Seventy-two hours after transfection, cells were treated with the indicated doses of doxorubicin for 2 hours and cell viability was analyzed 72 hours after drug exposure. D, HCC1937 or SKBR7 cells were transfected with siRNAs as in C and treated 72 hours later with 5 μmol/L etoposide (Etop) or doxorubicin (Doxo) for 1 hour, lysed, and analyzed with SDS-PAGE and Western blotting analysis. Quantifications in C and D are mean + SD of independent triplicate experiments. Statistical significance was calculated compared with control (*, $P < 0.05$; **, $P < 0.01$; ***, $P < 0.001$).

C9orf82 depletion desensitizes cells to etoposide. Our data indicate that C9orf82 is a nuclear protein that controls the rate of DNA DSB repair after exposure to Topo II poisons. Doxorubicin itself slows down DNA repair, which might explain why the resistance is most prominent following etoposide exposure. Given that most etoposide-induced DNA DSBs are repaired by NHEJ (45), C9orf82 may impinge on this arm of the DNA repair pathway, but how is currently unclear. C9orf82 is found mutated in 7% to 11% of glioblastoma tumors (13, 46), which makes it a potential prognostic factor in the treatment of such patients with etoposide. However, further studies integrating clinical response data with mutational analyses are required to substantiate this possibility.

Besides this relatively unknown protein, we characterized the role of the SWI/SNF complex in the resistance to TopoII poisons. The SWI/SNF complex is mutated in around 20% of human tumors (14) and has been linked to tumor suppression (37). SWI/SNF complex subunits like SMARCB1 control the loading of Topo IIα onto the DNA and hereby determine the extent of DNA damage induced following exposure to Topo II poisons. SMARCB1-depleted cells therefore have less DNA breaks when exposed to Topo II poisons and thus a growth advantage. As many of the tumors that harbor mutations in the SWI/SNF complex are treated with Topo II poisons, drug resistance could arise even when Topo IIα is expressed.

Several lines of evidence support this notion in patients. For example, SMARCB1 is mutated in 90% to 100% of the rhabdoid tumors (47, 48), a very aggressive childhood tumor that is unresponsive to doxorubicin (49). Also, epithelioid sarcoma patients harboring deletions for SMARCB1 have a higher chance of relapse following treatment protocols that usually includes Topo II poisons (39). Furthermore, we explored a data set of TNBC patients where both gene expression and treatment responses were documented. A correlation between treatment response and expression of SWI/SNF subunits SMARCB1 and SMARCA4 was observed within patients treated with doxorubicin and cyclophosphamide. No correlation was observed for SMARCE1 and ARID1a, which could be because SMARCE1 is not a part of the core complex essential for activity and ARID1a has

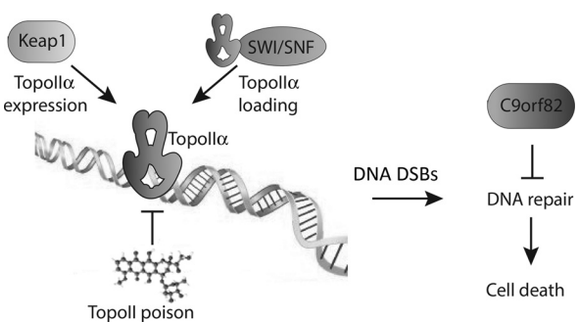

Figure 7.
Model of SWI/SNF, Keap1, and C9orf82 regulating different phases of Topo II poison-induced DNA break formation and DDR. Topo II poisons like doxorubicin induce DNA DSBs by trapping Topo II on the DNA. If not sufficiently repaired, this leads to cell death. Keap1 controls the expression of Topo IIα, while SWI/SNF regulates the loading and hereby activity of Topo IIα. Loss of these genes therefore attenuates DNA DSB formation by Topo II poisons. In the next phase of the DNA breaks and repair cycle, C9orf82 controls DNA repair. Loss of C9orf82 accelerates DNA repair, reducing cell death induced by Topo II poisons.

Published OnlineFirst August 10, 2015; DOI: 10.1158/0008-5472.CAN-15-0380

redundancy with ARID1b (29), or because the expression of these factors is not the limiting factor for the complex to function. Given the resistance to doxorubicin observed in our cell culture experiments, these data suggest that patients with low or depleted SWI/SNF expression should not be treated with doxorubicin, but rather with aclarubicin or topotecan, which are drugs that work through a different mechanism and that do not show any cross resistance in our experiments.

In conclusion, we identified and characterized three factors controlling sensitivity to the frequently used anticancer drugs doxorubicin and etoposide. Keap1, C9orf82, and the SWI/SNF chromatin remodeling complex all act by affecting DNA DSB formation or repair following exposure to these drugs. Mutations in these genes are frequently observed in human tumors and expected to yield tumors that are resistant to these drugs, as we show for TNBC patients. Profiling patients for mutations in these genes can further stratify treatment options as nonresponding patients can be selected for other treatments rather than given ineffective treatment containing Topo II poisons.

Disclosure of Potential Conflicts of Interest

T.R. Brummelkamp has ownership interest (including patents) in Haplogen GmbH. No potential conflicts of interest were disclosed by the other authors.

Authors' Contributions

Conception and design: R.H. Wijdeven, B. Pang, J. Neefjes
Development of methodology: R.H. Wijdeven, B. Pang
Acquisition of data (provided animals, acquired and managed patients, provided facilities, etc.): R.H. Wijdeven, B. Pang, X. Qiao, V. Blomen, E.H. Lips, L. Janssen
Analysis and interpretation of data (e.g., statistical analysis, biostatistics, computational analysis): R.H. Wijdeven, B. Pang, S.Y. van der Zanden, V. Blomen, M. Hoogstraat, E.H. Lips, L. Wessels, T.R. Brummelkamp
Writing, review, and/or revision of the manuscript: R.H. Wijdeven, B. Pang, S.Y. van der Zanden, M. Hoogstraat, E.H. Lips, J. Neefjes
Administrative, technical, or material support (i.e., reporting or organizing data, constructing databases): R.H. Wijdeven
Study supervision: J. Neefjes

Acknowledgments

The authors thank the NKI Genomics Core Facility for help with the sequencing data and the NKI Flow Cytometry Facility and the NKI Digital Microscopy Facility for support. The authors also thank Piet Borst and Ilana Berlin for critically reading the article and Jelle Wesseling and members of the Neefjes lab for fruitful discussions.

Grant Support

This work was supported by the Institute for Chemical Immunology, an NWO Gravitation project funded by the Ministry of Education, Culture and Science of the government of the Netherlands. This work was further supported by grants from the Netherlands Organization of Scientific Research NWO and an ERC Advanced Grant.

The costs of publication of this article were defrayed in part by the payment of page charges. This article must therefore be hereby marked *advertisement* in accordance with 18 U.S.C. Section 1734 solely to indicate this fact.

Received February 6, 2015; revised June 16, 2015; accepted July 14, 2015; published OnlineFirst August 10, 2015.

References

1. Pommier Y. Drugging topoisomerases: lessons and challenges. ACS Chem Biol 2013;8:82–95.
2. Borst P. Cancer drug pan-resistance: pumps, cancer stem cells, quiescence, epithelial to mesenchymal transition, blocked cell death pathways, persisters or what? Open Biol 2012;2:120066.
3. Pang B, Qiao X, Janssen L, Velds A, Groothuis T, Kerkhoven R, et al. Drug-induced histone eviction from open chromatin contributes to the chemotherapeutic effects of doxorubicin. Nat Commun 2013;4:1908.
4. Yang F, Kemp ChristopherÂ J, Henikoff S. Doxorubicin enhances nucleosome turnover around promoters. Curr Biol 2013;23:782–87.
5. Pang B, de Jong J, Qiao X, Wessels LF, Neefjes J. Chemical profiling of the genome with anti-cancer drugs defines target specificities. Nat Chem Biol 2015;11:472–80.
6. Callaghan R, Luk F, Bebawy M. Inhibition of the multidrug resistance P-glycoprotein: time for a change of strategy? Drug Metab Dispos 2014;42:623–31.
7. Burgess DJ, Doles J, Zender L, Xue W, Ma B, McCombie WR, et al. Topoisomerase levels determine chemotherapy response *in vitro* and *in vivo*. Proc Natl Acad Sci U S A 2008;105:9053–8.
8. Bouwman P, Jonkers J. The effects of deregulated DNA damage signalling on cancer chemotherapy response and resistance. Nat Rev Cancer 2012;12:587–98.
9. Zoppoli G, Regairaz M, Leo E, Reinhold WC, Varma S, Ballestrero A, et al. Putative DNA/RNA helicase Schlafen-11 (SLFN11) sensitizes cancer cells to DNA-damaging agents. Proc Natl Acad Sci U S A 2012;109:15030–5.
10. Carette JE, Guimaraes CP, Wuethrich I, Blomen VA, Varadarajan M, Sun C, et al. Global gene disruption in human cells to assign genes to phenotypes by deep sequencing. Nat Biotechnol 2011;29:542–6.
11. Shibata T, Kokubu A, Gotoh M, Ojima H, Ohta T, Yamamoto M, et al. Genetic alteration of Keap1 confers constitutive Nrf2 activation and resistance to chemotherapy in gallbladder cancer. Gastroenterology 2008;135:1358–68, 68.e1–4.
12. Singh A, Misra V, Thimmulappa RK, Lee H, Ames S, Hoque MO, et al. Dysfunctional KEAP1-NRF2 interaction in non-small-cell lung cancer. PLoS Med 2006;3:e420.
13. Network CGAR. Comprehensive genomic characterization defines human glioblastoma genes and core pathways. Nature 2008;455:1061–8.
14. Kadoch C, Hargreaves DC, Hodges C, Elias L, Ho L, Ranish J, et al. Proteomic and bioinformatic analysis of mammalian SWI/SNF complexes identifies extensive roles in human malignancy. Nat Genet 2013;45:592–601.
15. Carette JE, Raaben M, Wong AC, Herbert AS, Obernosterer G, Mulherkar N, et al. Ebola virus entry requires the cholesterol transporter Niemann-Pick C1. Nature 2011;477:340–3.
16. Johnson JP, Demmer-Dieckmann M, Meo T, Hadam MR, Riethmuller G. Surface antigens of human melanoma cells defined by monoclonal antibodies. I. Biochemical characterization of two antigens found on cell lines and fresh tumors of diverse tissue origin. Eur J Immunol 1981;11:825–31.
17. Hsu PD, Scott DA, Weinstein JA, Ran FA, Konermann S, Agarwala V, et al. DNA targeting specificity of RNA-guided Cas9 nucleases. Nat Biotechnol 2013;31:827–32.
18. Wang H, Yang H, Shivalila CS, Dawlaty MM, Cheng AW, Zhang F, et al. One-step generation of mice carrying mutations in multiple genes by CRISPR/Cas-mediated genome engineering. Cell 2013;153:910–8.
19. Auer TO, Duroure K, De Cian A, Concordet JP, Del Bene F. Highly efficient CRISPR/Cas9-mediated knock-in in zebrafish by homology-independent DNA repair. Genome Res 2014;24:142–53.
20. Neijenhuis S, Verwijs-Janssen M, Kasten-Pisula U, Rumping G, Borgmann K, Dikomey E, et al. Mechanism of cell killing after ionizing radiation by a dominant negative DNA polymerase beta. DNA Repair 2009;8:336–46.
21. Paul P, van den Hoorn T, Jongsma ML, Bakker MJ, Hengeveld R, Janssen L, et al. A Genome-wide multidimensional RNAi screen reveals pathways controlling MHC class II antigen presentation. Cell 2011;145:268–83.
22. de Ronde JJ, Lips EH, Mulder L, Vincent AD, Wesseling J, Nieuwland M, et al. SERPINA6, BEX1, AGTR1, SLC26A3, and LAPTM4B are markers of

resistance to neoadjuvant chemotherapy in HER2-negative breast cancer. Breast Cancer Res Treat 2013;137:213–23.
23. Trapnell C, Pachter L, Salzberg SL. TopHat: discovering splice junctions with RNA-Seq. Bioinformatics 2009;25:1105–11.
24. Anders S, Pyl PT, Huber W. HTSeq-a Python framework to work with high-throughput sequencing data. Bioinformatics 2015;31:166–9.
25. Love MI, Huber W, Anders S. Moderated estimation of fold change and dispersion for RNA-Seq data with DESeq2. Genome Biol 2014;15:550.
26. Benjamin RS, Riggs CE, Bachur NR. Plasma pharmacokinetics of adriamycin and its metabolites in humans with normal hepatic and renal function. Cancer Res 1977;37:1416–20.
27. Ohta T, Iijima K, Miyamoto M, Nakahara I, Tanaka H, Ohtsuji M, et al. Loss of Keap1 function activates Nrf2 and provides advantages for lung cancer cell growth. Cancer Res 2008;68:1303–9.
28. Wang XJ, Sun Z, Villeneuve NF, Zhang S, Zhao F, Li Y, et al. Nrf2 enhances resistance of cancer cells to chemotherapeutic drugs, the dark side of Nrf2. Carcinogenesis 2008;29:1235–43.
29. Hohmann AF, Vakoc CR. A rationale to target the SWI/SNF complex for cancer therapy. Trends Genet 2014;30:356–63.
30. Tsang WP, Chau SP, Kong SK, Fung KP, Kwok TT. Reactive oxygen species mediate doxorubicin induced p53-independent apoptosis. Life Sci 2003;73:2047–58.
31. Rogalska A, Koceva-Chyla A, Jozwiak Z. Aclarubicin-induced ROS generation and collapse of mitochondrial membrane potential in human cancer cell lines. Chem Biol Interact 2008;176:58–70.
32. Konstantinopoulos PA, Spentzos D, Fountzilas E, Francoeur N, Sanisetty S, Grammatikos AP, et al. Keap1 mutations and Nrf2 pathway activation in epithelial ovarian cancer. Cancer Res 2011;71:5081–9.
33. Sporn MB, Liby KT. NRF2 and cancer: the good, the bad and the importance of context. Nat Rev Cancer 2012;12:564–71.
34. Miyoshi Y, Kurosumi M, Kurebayashi J, Matsuura N, Takahashi M, Tokunaga E, et al. Predictive factors for anthracycline-based chemotherapy for human breast cancer. Breast Cancer 2010;17:103–9.
35. Sinha BK, Haim N, Dusre L, Kerrigan D, Pommier Y. DNA strand breaks produced by etoposide (VP-16,213) in sensitive and resistant human breast tumor cells: implications for the mechanism of action. Cancer Res 1988;48:5096–100.
36. Zhang Y, Johansson E, Miller ML, Janicke RU, Ferguson DJ, Plas D, et al. Identification of a conserved anti-apoptotic protein that modulates the mitochondrial apoptosis pathway. PLoS ONE 2011;6:e25284.
37. Dykhuizen EC, Hargreaves DC, Miller EL, Cui K, Korshunov A, Kool M, et al. BAF complexes facilitate decatenation of DNA by topoisomerase IIalpha. Nature 2013;497:624–7.
38. Hornick JL, Dal Cin P, Fletcher CD. Loss of INI1 expression is characteristic of both conventional and proximal-type epithelioid sarcoma. Am J Surg Pathol 2009;33:542–50.
39. Gasparini P, Facchinetti F, Boeri M, Lorenzetto E, Livio A, Gronchi A, et al. Prognostic determinants in epithelioid sarcoma. Eur J Cancer 2011;47:287–95.
40. Lee DF, Kuo HP, Liu M, Chou CK, Xia W, Du Y, et al. KEAP1 E3 ligase-mediated downregulation of NF-kappaB signaling by targeting IKKbeta. Mol Cell 2009;36:131–40.
41. Fan W, Tang Z, Chen D, Moughon D, Ding X, Chen S, et al. Keap1 facilitates p62-mediated ubiquitin aggregate clearance via autophagy. Autophagy 2010;6:614–21.
42. Zhan L, Zhang H, Zhang Q, Woods CG, Chen Y, Xue P, et al. Regulatory role of KEAP1 and NRF2 in PPARgamma expression and chemoresistance in human non-small-cell lung carcinoma cells. Free Radic Biol Med 2012;53:758–68.
43. Lawrence MS, Stojanov P, Mermel CH, Robinson JT, Garraway LA, Golub TR, et al. Discovery and saturation analysis of cancer genes across 21 tumour types. Nature 2014;505:495–501.
44. Barbano R, Muscarella LA, Pasculli B, Valori VM, Fontana A, Coco M, et al. Aberrant Keap1 methylation in breast cancer and association with clinicopathological features. Epigenetics 2013;8:105–12.
45. Quennet V, Beucher A, Barton O, Takeda S, Lobrich M. CtIP and MRN promote non-homologous end-joining of etoposide-induced DNA double-strand breaks in G1. Nucleic Acids Res 2011;39:2144–52.
46. Brennan CW, Verhaak RG, McKenna A, Campos B, Noushmehr H, Salama SR, et al. The somatic genomic landscape of glioblastoma. Cell 2013;155:462–77.
47. Versteege I, Sevenet N, Lange J, Rousseau-Merck MF, Ambros P, Handgretinger R, et al. Truncating mutations of hSNF5/INI1 in aggressive paediatric cancer. Nature 1998;394:203–6.
48. Margol AS, Judkins AR. Pathology and diagnosis of SMARCB1-deficient tumors. Cancer Genet 2014;207:358–64.
49. Tomlinson GE, Breslow NE, Dome J, Guthrie KA, Norkool P, Li S, et al. Rhabdoid tumor of the kidney in the National Wilms' Tumor Study: age at diagnosis as a prognostic factor. J Clin Oncol 2005;23:7641–5.

Published OnlineFirst August 10, 2015; DOI: 10.1158/0008-5472.CAN-15-0380

Cancer Research
The Journal of Cancer Research (1916–1930) | The American Journal of Cancer (1931–1940)

AACR American Association for Cancer Research

Genome-Wide Identification and Characterization of Novel Factors Conferring Resistance to Topoisomerase II Poisons in Cancer

Ruud H. Wijdeven, Baoxu Pang, Sabina Y. van der Zanden, et al.

Cancer Res 2015;75:4176-4187. Published OnlineFirst August 10, 2015.